Inorganic Chemistry

Article

pubs.acs.org/IC

Sequential Picosecond Isomerizations in a Photochromic Ruthenium Sulfoxide Complex Triggered by Pump-Repump-Probe Spectroscopy

Albert W. King,[†] Yuhuan Jin,[†] James T. Engle,[‡] Christopher J. Ziegler,[‡] and Jeffrey J. Rack*[,†]

[†]Department of Chemistry and Biochemistry, Nanoscale and Quantum Phenomena Institute, Ohio University, Clippinger Laboratories, Athens, Ohio 45701, United States

[‡]Department of Chemistry, Knight Chemical Laboratory, University of Akron, Akron, Ohio 44325, United States

Supporting Information

ABSTRACT: The complex $[Ru(bpy)_2(bpSO)](PF_6)_2$, where bpy is 2,2′-bipydine and bpSO is 1,2-bis(phenylsulfinyl)ethane, exhibits three distinct isomers which are accessible upon metal-to-ligand charge-transfer (MLCT) irradiation. This complex and its parent, $[Ru(bpy)_2(bpte)](PF_6)_2$, where bpte is 1,2-bis(phenylthio)ethane, have been synthesized and characterized by UV−visible spectroscopy, NMR, X-ray crystallography, and femtosecond transient absorption spectroscopy. A novel method of 2-color Pump-Repump-Probe spectroscopy has been employed to investigate all three isomers of the bis-sulfoxide complex. This method allows for observation of the isomerization dynamics of sequential isomerizations of each sulfoxide from MLCT irradiation of the S,S-bonded complex to ultimately form the O,O-bonded metastable complex. One-dimensional (1-D) and two-dimensional (2-D) (COSY, NOESY, and TOCSY) ^{1}H NMR data show the thioether and ground state S,S-bonded sulfoxide complexes to be rigorously C_2 symmetric and are consistent with the crystal structures. Transient absorption spectroscopy reveals that the S,S to S,O isomerization occurs with an observed time constant of 56.8 (±7.4) ps. The S,O to O,O isomerization time constant was found to be 59 (±4) ps by pump-repump-probe spectroscopy. The composite S,S- to O,O-isomer quantum yield is 0.42.

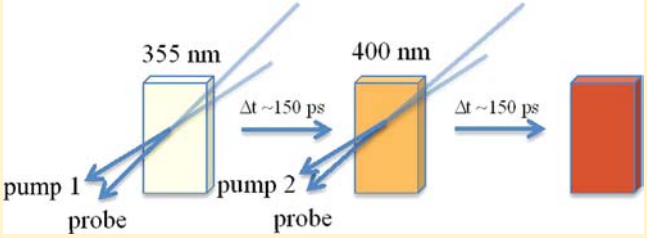

INTRODUCTION

Photochromic compounds efficiently convert photonic energy to potential energy for selective excited state bond-breaking and bond-making reactions. Such compounds have been employed for creating molecular information storage strategies,[1−3] for controlling biological activity,[4,5] and for developing functional materials.[6,7] More recently, photochromic compounds, by virtue of the distinct electronic and molecular structures exhibited by isomeric forms, have displayed striking photomechanical properties when incorporated within polymeric materials.[8−10] The fundamental concept connecting these two fields is the coupling of nuclear motion with the electronic wave function and the amplification of this motion onto a larger scale. Thus, the identification of new complexes with large and rapid excited state displacements advances both our understanding of this effect as well as the development of novel shape-changing photoactive materials.[11]

We have developed a class of photochromic ruthenium sulfoxide complexes whose mode of action is an excited state S→O and O→S isomerization of a bound sulfoxide ligand,[12−14] which expands the growing field of phototriggered linkage isomerization.[15−23] These sulfoxide isomerization events have been shown to occur on the picosecond time scale with substantial quantum yields. The change in ligation from S to O leads to significant changes in absorption, typically on the order of 5000 cm^{-1}. Moreover, these compounds feature large Huang−Rhys parameters indicative of strong coupling of excited state nuclear motion with the electronic wave function.[24] There have been a number of computational reports describing phototriggered sulfoxide isomerizations[25−27] and thermal sulfoxide isomerizations.[28−30] A characteristic of transition metal photochromes of this type is the facile introduction of multiple sulfoxide ligands within the inner coordination sphere.[31,32] Multiple sulfoxide ligands expand the color response of the photochrome and introduce questions regarding which sulfoxide isomerizes first as well as how to control these reactions. In this work, we demonstrate sequential picosecond isomerizations in a bis-sulfoxide complex by 2-color pump-repump-probe transient absorption spectroscopy.

EXPERIMENTAL SECTION

Materials. The reagents, $RuCl_3{\cdot}xH_2O$ and silver hexafluorophosphate ($AgPF_6$), were purchased from Strem. The ligand 1,2-bis(phenylthio)ethane (bpte) was purchased from Alfa Aesar. The oxidizing agent 3-chloroperoxybenzoic acid (*m*-cpba) and 2-methyltetrahydrofuran (2-Me-THF) were purchased from Sigma-Aldrich, as was HPLC grade propylene carbonate (PC) which was used as received. ACS grade solvents were purchased from Fisher Scientific and used without further purification. Deuterated d_6-acetone was obtained from Cambridge Isotope Laboratories, Inc. The starting material $Ru(bpy)_2Cl_2{\cdot}2H_2O$ (bpy is 2,2′-bipyridine) was prepared in

Received: November 14, 2012
Published: February 6, 2013

   dx.doi.org/10.1021/ic302489a | *Inorg. Chem.* 2013, 52, 2086−2093

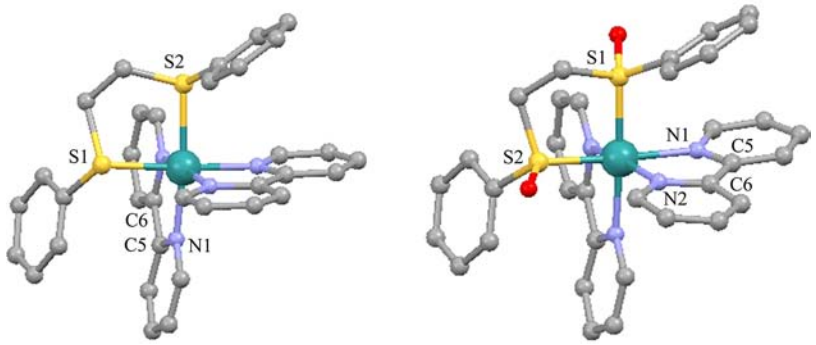

Figure 1. Molecular structures of $[Ru(bpy)_2(bpte)]^{2+}$ (left) and $[Ru(bpy)_2(bpSO)]^{2+}$ (right), with selected atom labels. Hydrogen atoms have been omitted for clarity. The full atom labeling is found in the Supporting Information.

accord with the literature procedure.[33] Elemental analysis was performed by Atlantic Microlab, Inc. of Norcross, Georgia, U.S.A.

Synthesis. *$[Ru(bpy)_2(bpte)](PF_6)_2$.* The named complex was synthesized by modification of a literature procedure.[34] Dark purple $Ru(bpy)_2Cl_2{\cdot}2H_2O$ (501 mg, 0.962 mmol) was dissolved in 20 mL of nitrogen (N_2) deaerated 1,2-dichloroethane with $AgPF_6$ (490 mg, 1.94 mmol). To this solution bpte (475 mg, 1.93 mmol) was added, and the reaction mixture was brought to reflux while stirring under a nitrogen atmosphere for 3 h, during which time the solution transitioned to a yellow-orange color. Excess $AgPF_6$ (230 mg, 0.910 mmol) was added, and the reaction mixture continued to reflux for 2 h, turning bright yellow by the end of the reaction. The solution was cooled to room temperature and further cooled to −30 °C overnight to facilitate the precipitation of AgCl. After cooling, the solution was filtered through a fine frit to remove AgCl, and the precipitate was washed with approximately 2 mL of acetonitrile. Solvent was removed from the filtrate by rotary evaporation, and the product was dried on a Schlenk line overnight. The yellow product was partially reconstituted in approximately 4 mL of methanol and precipitated from the solution by the addition of 40 mL of diethyl ether. The product was collected by vacuum filtration and reprecipitated from methanol by the addition of diethyl ether twice more to yield the product as a bright yellow powder. Characterization of the complex is consistent with the previous literature report.[34] Single crystals suitable for X-ray diffraction were produced by slow evaporation of methanol from a concentrated solution of the complex. Yield: 754 mg (82%). UV−vis (propylene carbonate) λ_{max} = 404 nm (5300 M^{-1} cm^{-1}). Emission (77 K, 4:1 2-Me-THF:PC) λ_{em} = 545 nm. ^1H NMR (d_6-acetone, 300 MHz): δ 9.89 (d, 2H, J = 5.5 Hz), 8.31 (m, 4H), 8.25 (t, 2H, J = 7.7 Hz), 8.08 (m, 4H), 8.01 (t, 2H, J = 6.6 Hz), 4.14 (d, 2H), 3.49 (d, 2H). Elemental Analysis: Calculated for $[Ru(C_{10}H_8N_2)_2(C_{14}H_{14}S_2)](PF_6)_2{\cdot}H_2O$: C, 42.20%, H, 3.33%, N, 5.79%. Found: C, 42.27%, H, 3.12%, N, 5.83%.

$[Ru(bpy)_2(bpSO)](PF_6)_2$. Oxidation of $[Ru(bpy)_2(bpte)](PF_6)_2{\cdot}H_2O$ (201 mg, 0.208 mmol) to produce the sulfoxide complex was accomplished with *m*-cpba (390 mg, 2.26 mmol) in 18 mL of 1,2-dichloroethane deareated with nitrogen for 10 days at 5 °C. The solution was vacuum filtered through a fine frit to remove any unreacted material, and solvent was removed from the filtrate by rotary evaporation. The resulting solid was then dried on a Schlenk line overnight, reconstituted in approximately 5 mL of methanol and precipitated upon the addition of approximately 40 mL of diethyl ether. The precipitate was isolated by vacuum filtration and washed with an additional 30 mL of diethyl ether to yield a pale yellow powder. Single crystals suitable for X-ray diffraction were produced by slow evaporation of methanol from a concentrated solution of the complex. Yield: 174 mg (85%). UV−vis (propylene carbonate) S,S-λ_{max} = 335 nm (7500 M^{-1} cm^{-1}). Emission (77 K, 4:1 2-Me-THF:PC) λ_{em} = 454 nm. ^1H NMR (d_6-acetone, 300 MHz): δ 10.15 (d, 2H, J = 5.4 Hz), 8.39 (m, 6H), 8.23 (t, 2H, J = 7.8 Hz), 8.11 (m, 2H), 7.75 (d, 2H, J = 5.5 Hz), 7.64 (t, 2H, J = 6.6 Hz), 7.56 (t, 2H, J = 7.6 Hz), 7.28 (t, 4H, J = 7.9 Hz), 7.12 (d, 4H, J = 8.2 Hz), 4.88 (d, 2H), 4.66 (d, 2H). Elemental Analysis: Calculated for $[Ru(C_{10}H_8N_2)_2(C_{14}H_{14}O_2S_2)](PF_6)_2$: C, 41.60%, H, 3.07%, N, 5.71%. Found: C, 41.86%, H, 3.00%, N, 5.76%.

Instrumentation. One dimensional (1-D) and two-dimensional (2-D) ^1H NMR spectra were collected on a 300 MHz Bruker AG spectrometer. All signals are referenced to a residual signal from deuterated solvent (d_6-acetone).

Single crystal X-ray diffraction data were collected at 100 K (Bruker KRYOFLEX) on a Bruker SMART APEX CCD-based X-ray diffractometer system equipped with a Mo-target X-ray tube (λ = 0.71073 Å). The detector was placed at a distance of 5.009 cm from the crystal. Crystals were placed in paratone oil upon removal from the mother liquor and mounted on a plastic loop in the oil. Integration and refinement of crystal data were done using the Bruker SAINT software package and Bruker SHELXTL (version 6.1) software package, respectively. Absorption correction was completed by using the SADABS program.

Bulk absorption spectra were collected on an Agilent 8453 UV−visible spectrometer in nitrogen deaerated propylene carbonate. A 1 cm quartz cuvette sealed by a rubber septum was used. Irradiation of the sample was performed using a Nd:YAG Continuum SURELITE laser pulsing 355 nm at 1.00 kV at 10 Hz.

The femtosecond system employed to collect ultrafast data in the standard pump-probe experiment has been previously reported.[35] A bulk solution of approximately 50 mL of deaerated PC was pumped through a 2 mm quartz cuvette by a fluid pump (Lab Pump Jr., model RHSY by Fluid Metering, Inc., Syosset, NY) at a flow rate of approximately 7.2 mL/min. Kinetic data were fit using Surface Xplorer Pro 1.1.5 by Ultrafast Systems, LLC. Data correction was achieved by background subtraction, chirp correction, and t_0 correction using this software. The kinetics were fit using the global analysis function in Surface Xplorer Pro 1.1.5 software.

The ultrafast pump-probe system was modified to achieve the pump-repump-probe experiment described below. In the standard pump-probe experiment, the probe beam is directed onto a 95/5 beamsplitter with the minority component reflected into the Helios and ultimately onto a CaF_2 crystal for white light generation. Typically, the 95% portion is dumped. We employed this portion for the second pump beam by passing it through a frequency doubling crystal, and onto a mirror with an adjustable stage. The beam was then directed though a chopper to discriminate every other pulse, identical to the first pump beam, and then onto the sample. The moving mirror allows for adjustment of the pump delay relative to the first pump beam. The photochemical solution employed in this experiment is prepared as that for the pump-probe experiment and data are worked up similarly, excepting that the data are separated at approximately 150 ps before the kinetics are fit for the respective data before and after the 400 nm pulse. Initial background subtraction, chirp correction, and t_0 correction are initially applied to the full data set; the chirp correction is derived from fits of solvent excited at 355 nm. Background subtraction, chirp correction, and t_0 correction are again applied to fit the data after the 400 nm pulse; this chirp correction is derived from fits of solvent excited at 400 nm 154 ps after a 355 nm pulse.

dx.doi.org/10.1021/ic302489a | *Inorg. Chem.* 2013, 52, 2086−2093

RESULTS AND DISCUSSION

A. Structural Characterization. Shown in Figure 1 are the molecular structures of $[Ru(bpy)_2(bpte)]^{2+}$ and $[Ru(bpy)_2(bpSO)]^{2+}$, where bpy is 2,2′-bipyridine, bpte is 1,2-bis(phenylthio)ethane, and bpSO is 1,2-bis(phenylsulfinyl)-ethane. Crystallographic data for both structures are displayed in Table 1. The dithioether complex, $[Ru(bpy)_2(bpte)]^{2+}$, is prepared by direct reaction of the dithioether ligand (bpte) with $Ru(bpy)_2Cl_2$.[34] Oxidation to produce $[Ru(bpy)_2(bpSO)]^{2+}$ is achieved by reaction of $[Ru(bpy)_2(bpte)]^{2+}$ with *m*-cpba in dichloroethane at 5 °C. Selected metrical parameters and angles are displayed in Table 2 (with the complete atom labeling scheme shown in Supporting Information, Figure S1). In comparison, the Ru−N bond distances and bipyridine chelate angles are similar and are consistent with literature reports.[36,37] For $[Ru(bpy)_2(bpte)]^{2+}$, both enantiomers are present in the unit cell (z = 4; space group $P\bar{1}$), which exhibit Ru−S bond distances of 2.342(4) and 2.338(3) Å as well as 2.331(4) and 2.351(3) Å. These data are consistent with the structural data found for $[Ru(phen)_2(bpte)]^{2+}$ (phen is 1,10-phenanthroline), where Ru−S bond distances are 2.401(2) and 2.307(2) Å.[38] The dithioether chelating ligand bite angle is 85.71(8)° in $[Ru(phen)_2(bpte)]^{2+}$ and 85.3(1)° and 85.3(1)° for the molecules in $[Ru(bpy)_2(bpte)]^{2+}$. Both $[Ru(bpy)_2(bpte)]^{2+}$ and $[Ru(phen)_2(bpte)]^{2+}$ appear to show intramolecular π-stacking interactions between the phenyl ring of the bpte ligand and one of the diimine ligands. In $[Ru(bpy)_2(bpte)]^{2+}$, the distance from the centroid of the phenyl ring (atoms C21−C26, inclusive; bonded to S1) to the closest bridgehead carbon of bipyridine (C6) is ∼3.43 Å, while the centroid of the phenyl ring (atoms C29−C34, inclusive; bonded to S2) to the closest bridgehead carbon of bipyridine (C15) is considerably longer at ∼3.98 Å, indicating that one of the phenyl rings is more parallel than the other. Indeed, the angle formed from the plane containing the phenyl ring (bonded to S2) and the plane formed from the bipyridine chelate (Ru−N3−C15−C16−N4) is 40.5°, whereas the corresponding angle between the other phenyl ring (bonded to S1) and bipyridine chelate is 17.6°. For $[Ru(phen)_2(bpte)]^{2+}$, the phenyl ring to closest bridgehead carbon representative distances are ∼3.40 Å for both phenyl rings. In $[Ru(phen)_2(bpte)]^{2+}$, the angles formed by the phenyl ring and the phenantroline ligand are 19.2° and 16.4°, respectively.

The molecular structure of $[Ru(bpy)_2(bpSO)]^{2+}$ displays Ru−N bond distances that are similar to those of the thioether compounds listed above. However, the Ru−S bond distance decreases to 2.258(2) and 2.248(2) Å, which is attributed to increased π-backbonding to the sulfoxide. These distances are significantly shorter than those observed in the related bis-sulfoxide complexes, $[Ru(bpy)_2(dmso)_2]^{2+}$ (dmso is dimethyl-sulfoxide), and $[Ru(bpy)_2(OSSO)]^{2+}$, (OSSO is dimethylbis-(methylsulfinylmethyl)silane), where Ru−S bond distances are all coincident at 2.293(1) Å.[31,32] The S−Ru−S angle of 85.91(6)° is the most acute in $[Ru(bpy)_2(bpSO)]^{2+}$, where this angle is 89.42(5)° and 92.92(4)° in $[Ru(bpy)_2(dmso)_2]^{2+}$ and $[Ru(bpy)_2(OSSO)]^{2+}$, respectively. There is much less variation in S═O bond distances in a comparison of these three structures.[31] For example, in $[Ru(bpy)_2(bpSO)]^{2+}$ the S═O bond distances are 1.477(5) and 1.480(5) Å, which are statistically identical to the S═O bond distance of 1.485(4) Å found in $[Ru(bpy)_2(OSSO)]^{2+}$. There are four unique S═O bond distances in $[Ru(bpy)_2(dmso)_2]^{2+}$ which are 1.473(4), 1.476(5), 1.480(4), and 1.479(4) Å. While the Ru−S bond distances in $[Ru(bpy)_2(bpSO)]^{2+}$ are shorter than those in the other sulfoxides complexes, the S═O bond distances are invariant. Given the structural differences in these complexes, one might expect dissimilarities in the photochemistry of these three complexes.

Similar to $[Ru(bpy)_2(bpte)]^{2+}$, there is clear evidence for π-stacking between the phenyl rings of the chelating sulfoxide ligand and bipyridine in $[Ru(bpy)_2(bpSO)]^{2+}$. Again, the phenyl rings are projected over the bipyridine ligand, with a phenyl ring centroid (atoms C29−C34 inclusive; adjacent to S2) to bridgehead C15 and C16 distance of ∼3.56 and ∼3.48 Å, respectively. These plane-to-plane distances are within the accepted range for intramolecular π-stacking distances, which are conventionally defined as ranging from ∼3.3 to 3.8 Å.[39] The phenyl ring centroid (atoms C21−C26 inclusive; adjacent to S1) to bridgehead C5 and C6 are displaced even further to

Table 1. Crystallographic Data for $[Ru(bpy)_2(bpte)](PF_6)_2$ and $[Ru(bpy)_2(bpSO)](PF_6)_2$

	$[Ru(bpy)_2(bpte)](PF_6)_2$	$[Ru(bpy)_2(bpSO)](PF_6)_2$
a (Å)	12.3925(18)	12.5563(3)
b (Å)	16.798(3)	12.5563(3)
c (Å)	17.277(3)	48.8146(12)
α (deg)	89.391(2)	90
β (deg)	81.720(2)	90
γ (deg)	89.849(2)	90
temperature (K)	100	100
wavelength (Å)	0.71073	1.54178
volume (Å)	3558.7(9)	7696.1(3)
space group	$P\bar{1}$	$P4(3)2(1)2$
M_r	949.75	981.75
density (g cm^{-3})	1.773	1.695
Z	4	8
μ (mm^{-1})	0.745	5.982
$F000$	1904.0	3936.0
h,k,l max	15,21,22	14,14,56
N_{ref}	14719	6378
T_{min}, T_{max}	0.859, 0.916	0.311,0.433
data completeness	0.949	1.62/0.95
θ (max)	27.000	65.900
R (reflections)	0.0851 (9583)	0.0569 (6303)
$wR2$ (reflections)	0.2432 (14719)	0.1509 (6378)
S	1.048	0.858
N_{par}	991	514

Table 2. Selected Bond Distances (Å) and Angles (deg)

	$[Ru(bpy)_2(bpte)]^{2+}$	$[Ru(bpy)_2(bpSO)]^{2+}$
Ru−S1	2.342(4)	2.248(2)
Ru−S2	2.338(3)	2.258(2)
Ru−N1	2.077(1)	2.108(6)
Ru−N2	2.079(1)	2.101(6)
Ru−N3	2.070(1)	2.108(6)
Ru−N4	2.070(1)	2.108(6)
S1−O1		1.480(5)
S2−O2		1.477(5)
N1−Ru−N2	78.7(4)	78.0(2)
N3−Ru−N4	78.2(4)	77.5(2)
S1−Ru−S2	85.3(1)	85.91(6)

dx.doi.org/10.1021/ic302489a | Inorg. Chem. 2013, 52, 2086−2093

~3.92 and ~3.82 Å, respectively, which approach the threshold for accepted plane-to-plane distances. Similar to the thioether complex, one of the phenyl rings is more parallel to its neighboring bipyridine than the other. The angle formed from the plane containing the phenyl ring (atoms C21−C26 inclusive; bonded to S1) and the plane containing the bipyridine chelate (Ru1−N1−C5−C6−N2) is 31.2°, whereas for the phenyl ring (atoms C29−C34 inclusive; bonded to S2) and the bipyridine chelate (Ru1−N3−C15−C16−N4) is more acute at 20.2°. In comparison to $[Ru(bpy)_2(bpte)]^{2+}$, while $[Ru(bpy)_2(bpSO)]^{2+}$ exhibits shorter Ru−S bonds, most of the other structural features do not change. The origin of the asymmetric interaction between the phenyl ring of the chelating sulfur ligands and the bipyridine is unclear.

The linear 1-D ^{1}H NMR data for $[Ru(bpy)_2(bpte)]^{2+}$ and $[Ru(bpy)_2(bpSO)]^{2+}$ display a single set of resonances for the bipyridine ligands, confirming the C_2 symmetry of the complex in solution. The correlation spectroscopy (COSY), nuclear Overhauser effect spectroscopy (NOESY), and total correlation spectroscopy (TOCSY) spectra of $[Ru(bpy)_2(bpSO)]^{2+}$ are shown in Supporting Information, Figures S2, S3, and S4. Of interest are the aliphatic resonances ascribed to the ethylene (C_2H_4) bridging the sulfur atoms in the chelating bpte or bpSO ligand. A complicated second-order coupling pattern (AA′BB′) is observed for these protons in $[Ru(bpy)_2(bpSO)]^{2+}$ with $^2J_{HH}$ (geminal) and three $^3J_{HH}$ coupling constants of 14.0 Hz and 4.0, 1.0, and 15.5 Hz, respectively. The Karplus equation relates $^3J_{HH}$ coupling constants on adjacent carbons to the dihedral angle and the electronegativity of the substituents on the carbon atoms. We employed Spin Works to simulate the spectra thus extracting $^2J_{HH}$ and $^3J_{HH}$ coupling constants. We then accessed the free program Sweet J (www.inmr.net) to determine the representative dihedral angle from the Karplus equation. The largest coupling constant corresponds to two protons with a dihedral angle of 180°. When $^3J_{HH}$ = 4.0 Hz this corresponds to an AA′ dihedral angle of 59°, indicating a similar structure in comparison to the solid state molecular structure which features a dihedral angle of 61° (Supporting Information, Figure S5). Analysis of the ^{1}H NMR spectrum of $[Ru(bpy)_2(bpte)]^{2+}$ yields similar results with $^2J_{HH}$ and three $^3J_{HH}$ coupling constants of 14.5 Hz and 3.3, 3.0, and 11.5 Hz, with an AA′ dihedral angle of 59°. Of course, the chelating nature of the ligand limits motion and the range of conformations available to this linkage in both complexes.

B. Electronic Spectroscopy. The absorption spectrum of ground state S,S-$[Ru(bpy)_2(bpSO)]^{2+}$ is shown in Figure 2. While the $\pi\rightarrow\pi^*$ bpy centered transition is observed at 319 nm, a less intense shoulder at ~335 nm is attributed to the Ru d$\pi\rightarrow$ bpy π^* charge transfer (CT) transition. The related bis-sulfoxide compounds $[Ru(bpy)_2(dmso)_2]^{2+}$, $[Os(bpy)_2(dmso)_2]^{2+}$, and $[Ru(bpy)_2(OSSO)]^{2+}$ feature metal-to-ligand charge-transfer (MLCT) maxima at 348, 355, and 350 nm, respectively, for the ground state S,S isomers.[31,32,40,41] For $[Ru(bpy)_2(dmso)_2]^{2+}$ and $[Ru(bpy)_2(OSSO)]^{2+}$, mechanistic studies reveal distinct S,O (λ_{max} ~400 nm) and O,O (λ_{max} ~360, ~490 nm) isomeric metastable states that are formed in consecutive reactions, which are uniquely identified by their absorption maxima. Importantly, the balance of quantum yields and rate constants permits preparation and isolation of each of these isomers. Irradiation of $[Ru(bpy)_2(bpSO)]^{2+}$ at 355 nm yields distinct changes in the absorption spectrum over time, with an initial absorbance appearing near 400 nm which subsequently gives rise to two new absorbance features

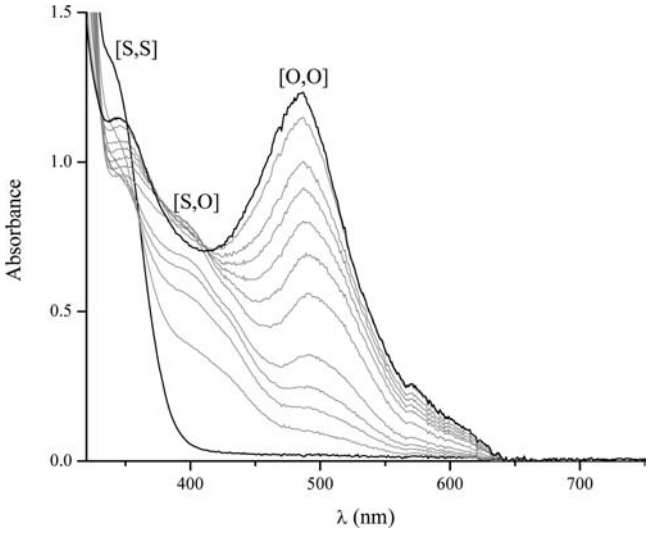

Figure 2. Electronic absorption spectra of $[Ru(bpy)_2(bpSO)](PF_6)_2$ in propylene carbonate and spectral changes following irradiation at 355 nm. The 500 nm absorbance rises throughout excitation, whereas the absorbance at 355 nm falls and then rises. In contrast, the absorbance at 400 rises and then falls during bulk photolysis.

appearing at 360 and 487 nm. There are two clear sets of isosbestic points for early time and later time irradiation, indicative of successive reactions. However, unlike $[Ru(bpy)_2(dmso)_2]^{2+}$, the bulk photolysis does not indicate a large rise in the concentration of the S,O-isomer, as the absorbance at 400 nm is never predominant in this series of spectra. These changes are consistent with two, sequential S→O isomerizations of the bound sulfoxide, as observed in $[Ru(bpy)_2(dmso)_2]^{2+}$.

Reversion of the O,O isomer to S,O- or S,S-$[Ru(bpy)_2(bpSO)]^{2+}$ is slow at room temperature. We found a rate constant of 5.2×10^{-6} s^{-1} for the O,O- to S,O-isomer by monitoring the spectral changes over a 12 h time span. Analysis of the spectra over a multiple week time range indicates that the S,S-isomer is ultimately formed. Irradiation of the O,O solution does seem to enhance the rate of reversion indicating an excited state pathway for the O,O→S,O isomerization. However, this quantum yield is exceptionally small ($\Phi_{O\rightarrow S} < 10^{-5}$). We are able to collect the ^{1}H NMR spectrum of O,O-$[Ru(bpy)_2(bpSO)]^{2+}$ in deuterated acetone. Similar to the S,S-isomer, the O,O-isomer appears C_2-symmetric with just 8 bipyridine resonances. Analysis of the C_2H_4 linker within in the disulfoxide chelate yields $^2J_{HH}$ and $^3J_{HH}$ coupling constants of 13.5 Hz and 4.0, 5.0, and 11.5 Hz, with an AA′ dihedral angle of 52°.

C. Transient Absorption Spectroscopy. We employed transient absorption spectroscopy to investigate the excited state dynamics and isomerization behavior of this compound. Moreover, we employed two pump beams of different color and delayed in time to independently excite the ground state S,S- and S,O-isomers in preparation of the O,O-isomer (Scheme 1). A recent report shows a similar technique focusing on the opening and closing of a single spiropyran photochrome.[42] The goal of this experiment is to observe sequential formation and conversion between three isomers of a single ruthenium complex, with each exhibiting a distinct absorption spectrum (Figure 2, Scheme 1).

Shown in Figure 3 are the picosecond transient absorption spectra of $[Ru(bpy)_2(bpSO)]^{2+}$. The transient at 1.0 ps features

dx.doi.org/10.1021/ic302489a | Inorg. Chem. 2013, 52, 2086−2093

Scheme 1. Sequential S→O Isomerizations in $[Ru(bpy)_2(bpSO)]^{2+}$

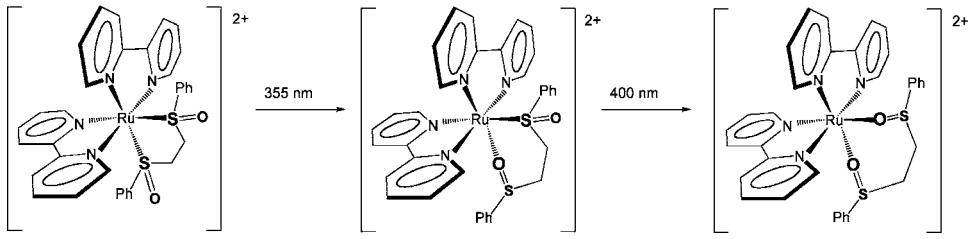

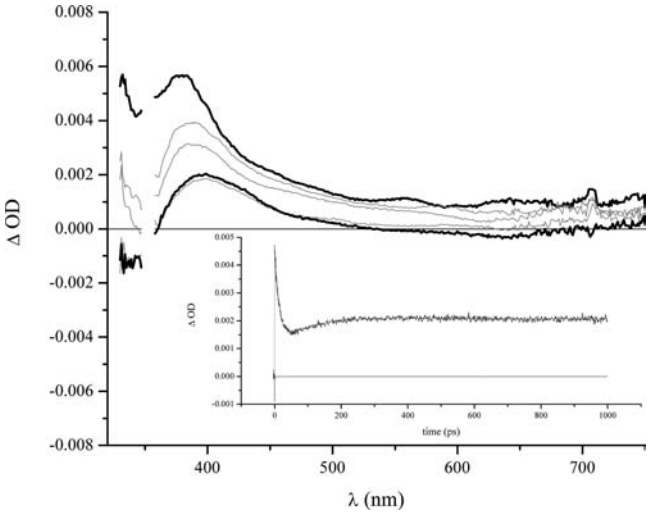

Figure 3. Transient absorption spectra of $[Ru(bpy)_2(bpSO)](PF_6)_2$ following 355 nm excitation. Evidence of laser pulse omitted for clarity. From top to bottom: 1 ps (bold, thick line), 5 ps, 10 ps, 150 ps, and 3000 ps (bold, thick line). Inset: kinetic trace obtained at 400 nm, showing the formation of the ground state S,O-isomer.

a sharp absorption at ~380 nm, which is assigned to a reduced bpy $\pi^*\rightarrow\pi^*$ transition and a broad, featureless absorption near 600 nm attributed to an excited state LMCT (Ligand-to-Metal CT) transition, both of which are associated with an MLCT excited state. Over the next 150 ps, the 600 nm feature collapses to zero ΔOD, and the 380 nm absorption shifts to the red and loses intensity. The absence of absorption in the red part of the spectrum indicates that a ground state molecule has formed. The new absorption at 400 nm is characteristic of a mixed S,O-bonded isomer seen in the study of both $[Ru(bpy)_2(dmso)_2]^{2+}$ and $[Ru(bpy)_2(OSSO)]^{2+}$, as well as in the bulk photolysis spectra of $[Ru(bpy)_2(bpSO)]^{2+}$ (Figure 2). Transient spectra obtained at longer time delays (3000 ps, bold spectrum) are identical to the 150 ps spectrum. Thus, the spectra suggest that a ground state isomer has been formed within 150 ps following excitation, which strongly resembles the mixed S,O-isomer observed in the study of similar bis-sulfoxide compounds. We assign this spectrum to the ground state mixed S,O-isomer.

Kinetic analysis from single wavelength kinetics at 380, 400, and 600 nm yields time constants of 0.11 (±0.09), 12.7 (±0.9), and 56.8 (±7.4) ps (Supporting Information, Figures S6, S7, and S8, respectively). The most rapid time constant is ascribed to ^{1}MLCT→^{3}MLCT intersystem crossing. The slowest time constant, 56.8 (±7.4) ps, is assigned to relaxation of a ^{3}MLCT state to the S,S-ground state isomer and isomerization to produce the ground state S,O-isomer. The 12.7 (±0.9) ps kinetic component is unique to ruthenium sulfoxide photochemistry and we have previously assigned this state to a new ^{3}MLCT state with a different bonding configuration of the sulfoxide relative to the initially formed ^{3}MLCT state.[35] Accordingly, we have termed this state the isomerizing state ($^3MLCT_{SS'}$), and it must exhibit a molecular configuration poised for isomerization. We also found a 1.16 (±0.29) ps kinetic component only at 380 nm, and this is attributed to solvent reorganization of the ^{3}MLCT state.[43] At present, we have found no reliable method to determine the quantum yields of the successive isomerizations. Indeed, while bulk photolysis at 355 (Figure 2) yields the desired S,O-isomer, it will also produce the O,O-isomer from the S,O-isomer. Thus, we are unable to independently monitor the relative concentrations of the three isomers as a function of irradiation time. However, if we assume the formation of the S,O-isomer to be >90% complete in 150 ps and a first order rate law, then the time constant for isomerization is ~60 ps, quite similar to our measured time constant of 56.8 ps. This represents the most rapid phototriggered isomerization time constant observed for any isomerizable metal sulfoxide. Moreover, it approaches the time constants of ring-closing in dithienylethenes, which occurs in the range of 1−10 ps.[44] Accordingly, this complex exhibits an efficient and rapid conversion of photonic energy to potential energy for selective excited state bond-breaking and bond-making reactions, making it an ideal candidate for the pump-repump-probe experiment described next.

D. Pump-Repump-Probe Spectroscopy. To investigate the second isomerization reaction, we incorporated a second pump beam at 400 nm into the spectrometer to excite the newly formed S,O-isomer produced from 355 nm excitation of the S,S-isomer. It is important to note that the S,S-isomer has no appreciable absorbance at 400 nm (Figure 2). The objective is to trigger the second isomerization that produces the O,O-isomer from the S,O-isomer (Scheme 1). Shown in Figure 4 is the kinetic trace at 510 nm. This wavelength corresponds to an absorption maximum for the O,O-isomer (Figure 2). In this trace, t = 0 is assigned to appearance of the 355 nm excitation pulse. The kinetics following this pulse correspond to the formation of the S,O-isomer as described above. After a delay of 154 ps, we introduced a second excitation pulse (400 nm) corresponding to MLCT excitation of the ground state S,O-isomer. The trace shows an immediate rise following appearance of the pulse. In the absence of the 400 nm excitation pulse, the trace at 510 nm remains flat for a time duration of >3000 ps, in accord with the formation of a ground state complex (S,O-isomer). The dramatic change of the trace is consistent with the formation of a species with a characteristic absorbance near 510 nm. Excitation of the S,S isomer with 400 nm results in no measurable transient features, presumably because of lack of absorbance of this isomer at this wavelength. The time constants associated with this trace (after

dx.doi.org/10.1021/ic302489a | Inorg. Chem. 2013, 52, 2086−2093

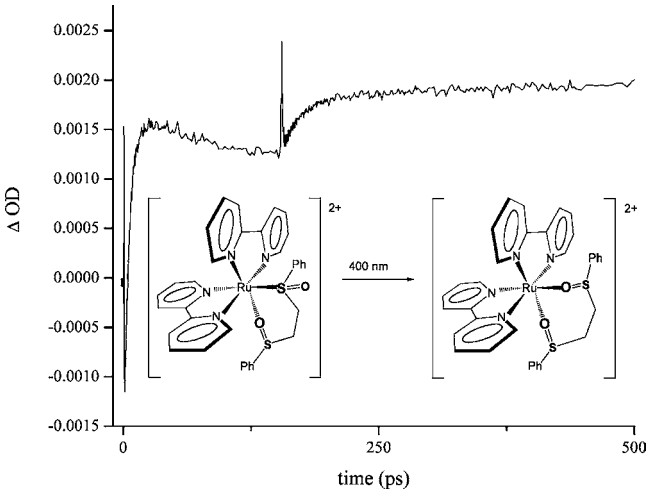

Figure 4. Kinetic trace obtained at 510 nm showing both 355 and 400 nm excitation. Inset shows the proposed reaction occurring following the second pump (λ_{exc} 400 nm).

400 nm excitation) are 0.11 (±0.003) and 28 (±3) ps (Supporting Information, Figure S9). Concomitantly, the kinetic trace at 600 nm, characteristic of the ^{3}MLCT excited state, reveals a biexponential decay to zero ΔOD with time constants of 1.7 (±0.2) and 59 (±4) ps (Supporting Information, Figure S10). The slower time constants are in good agreement with one another and are attributed to formation of the ground state O,O-isomer. We are uncertain of the origin of the ∼2 ps time constant observed at 600 nm. Slow solvent reorganization is not typically seen at this wavelength,[43] so it may be the appearance of an isomerizing state, similar to that observed in the S,S→S,O isomerization. These studies are among the first reports employing ultrafast multipulse techniques on photochromic compounds and, to our knowledge, the first involving a photochromic transition metal complex.[42,45]

It is interesting to note that each isomerization is efficient and that ground state isomers can be formed within 150−200 ps following excitation. We,[12] and others,[28,46,47] have found great variability in the time constants of sulfoxide isomerizations. For the phototriggered isomerizations in our class of compounds, $\tau_{S\rightarrow O}$ may vary by nearly 4 orders of magnitude, and we have also prepared compounds that do not isomerize at all.[48] We note that the compounds that show the greatest quantum yields and the most rapid velocities are those in which the sulfur is bonded to an sp^2-hyrbidized carbon of a phenyl ring. We do not yet know the exact role of the phenyl group, but the MLCT transition of ruthenium sulfoxides involves significant sulfur character,[27,49,50] and thus it is reasonable to expect modification of this transition (and excited state dynamics) through conjugation with the aromatic ring.

While the data show that the two sulfoxide ligands isomerize independently, they are structurally and symmetrically equivalent in the ground state S,S isomer (and presumably in the product O,O-isomer). Yet, in local C_2 symmetry (*z*-axis bisecting bpSO ligand), each d orbital will exhibit either A or B symmetry, and the bonding descriptions of each metal-sulfoxide moiety are unique. The first isomerization is determined by the interaction between the laser polarization and the molecular orientation. Further control over the fate of the complex can be introduced through removal of the C_2 symmetry operation, that is, by replacing bipyridine with a substituted bipyridine. Such asymmetric complexes will enable complete control over the isomerization sequence.

The kinetic data may be compiled within a single state diagram (Figure 5). Excitation of S,S-[Ru(bpy)$_2$(bpSO)]$^{2+}$ with

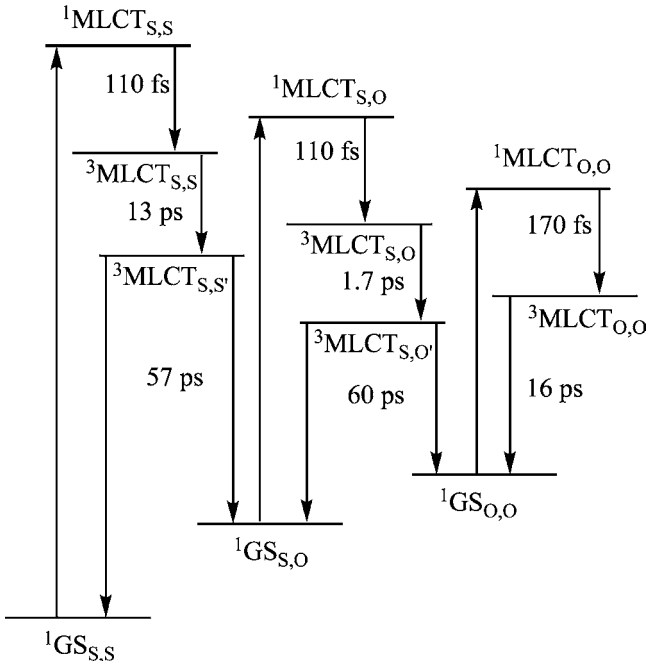

Figure 5. State diagram for [Ru(bpy)$_2$(bpSO)](PF$_6$)$_2$. Not depicted is the O,O- to S,O-isomer photochemical pathway.

355 nm yields the ^{1}MLCT$_{S,S}$ state, which rapidly converts to ^{3}MLCT$_{S,S}$, in accordance with literature reports. This state evolves to a new CT state termed ^{3}MLCT$_{S,S'}$ with a time constant of 13 ps. From this state the complex both relaxes to ground state (^{1}GS$_{SS}$) and isomerizes to the mixed S,O-bonded ground state isomer (^{1}GS$_{SO}$). Subsequent excitation of ^{1}GS$_{SO}$ by the pump-repump-probe technique described here with 400 nm produces the ^{1}MLCT$_{S,O}$ state, which efficiently intersystem crosses to ^{3}MLCT$_{S,O}$. Again, we observe the appearance of a new CT state with a time constant of 1.7 ps. Subsequent relaxation and isomerization occurs with a time constant of 60 ps. In the absence of quantum yield values for the isomerization, we are unable to precisely determine isomerization time constants for the individual steps. However, we have determined the composite quantum yield representing the conversion of S,S-[Ru(bpy)$_2$(bpSO)]$^{2+}$ to O,O-[Ru(bpy)$_2$(bpSO)]$^{2+}$ to be 0.42, a value indicative of the efficiency of the overall transformation.

It is interesting to compare the sequential isomerizations in [Ru(bpy)$_2$(bpSO)]$^{2+}$ to those in [Ru(bpy)$_2$(dmso)$_2$]$^{2+}$ and [Ru(bpy)$_2$(OSSO)]$^{2+}$, which reveals a number of distinguishing features. In [Ru(bpy)$_2$(dmso)$_2$]$^{2+}$, the mixed S,O-isomer is clearly visible in the bulk photolysis of the S,S isomer to ultimately produce the O,O isomer. For [Ru(bpy)$_2$(bpSO)]$^{2+}$, this isomer is hardly apparent and is never formed in large yield, suggesting that the quantum yield for isomerization of S,O to O,O must be more facile or efficient for [Ru(bpy)$_2$(bpSO)]$^{2+}$. Also, thermal reversion from the O,O isomer to the S,O isomer in both [Ru(bpy)$_2$(dmso)$_2$]$^{2+}$ and [Ru(bpy)$_2$(OSSO)]$^{2+}$ is much more rapid ($k \sim 10^{-4}$ s^{-1}), than that found for [Ru(bpy)$_2$(bpSO)]$^{2+}$ ($k \sim 10^{-6}$ s^{-1}). Indeed, in both [Ru(bpy)$_2$(dmso)$_2$]$^{2+}$ and [Ru(bpy)$_2$(OSSO)]$^{2+}$, the mixed

dx.doi.org/10.1021/ic302489a | *Inorg. Chem.* 2013, 52, 2086−2093

S,O-isomer may be produced, isolated, and investigated from ground state thermal reversion of the O,O isomer. For $[Ru(bpy)_2(dmso)_2]^{2+}$, both sulfoxide ligands are untethered from one another, and thus the first isomerization is likely to have a small influence on the second isomerization. In $[Ru(bpy)_2(OSSO)]^{2+}$, the two sulfoxides are tethered by a flexible 3 atom linker ($-CH_2Si(CH_3)_2CH_2-$). It is thus not unreasonable to expect that the first isomerization induces some small stress upon the second sulfoxide in a chelating bis-sulfoxide complex. The resultant strain may be large in $[Ru(bpy)_2(bpSO)]^{2+}$ where the mixed S,O-isomer is not easily formed during thermal reversion and reacts quickly with light to form the O,O-isomer. In this case, a hypothesis emerges that states that the first isomerization strains the chelate ring, resulting in a structural geometry poised for isomerization. At odds with this hypothesis is the expansion of the chelate ring from 5 to 6, which seemingly should reduce strain. However, we do not know how the remaining Ru−S bond is affected after the first isomerization, though it is safe to suggest that it strengthens or shortens as S-bonded sulfoxides are often considered π-acids. While speculative, the aggregate motion of Ru−S bond shortening with chelate twisting may lead to a conformation that is positioned for efficient and rapid isomerization.

CONCLUSION

This study represents our first attempt to phototrigger multiple sulfoxide isomerizations within a single complex. The data show that we are able to manipulate the isomerization state of a single compound by utilizing different wavelength pump beams. Specifically, we have employed a second excitation pulse to probe one of three ground states (S,O-isomer) along the lowest energy potential energy surface. Future studies will apply this technique to electronic excited states,[51,52] in particular the isomerizing state. Indeed, these studies are proceeding in our laboratory, with the objective of directing and controlling excited state reaction pathways with light.

ASSOCIATED CONTENT

Supporting Information

Selected kinetic traces, NMR data and X-ray crystallographic files. This material is available free of charge via the Internet at http://pubs.acs.org.

AUTHOR INFORMATION

Corresponding Author

*E-mail: rackj@ohio.edu.

Notes

The authors declare no competing financial interest.

ACKNOWLEDGMENTS

We thank Shadrick Paris for helpful discussions. This material is based upon work supported by the National Science Foundation under Grants CHE 0809699, CHE 0947031, and CHE 1112250.

ABBREVIATIONS

bpy, 2,2′-bipyridyl; bpSO, 1,2-bis(phenylsulfinyl)ethane; bpte, 1,2-bis(phenylsulfanyl)ethane; *m*-cpba, *m*-chloroperbenzoic acid; COSY, correlation spectroscopy; TOCSY, total correlation spectroscopy; NOESY, nuclear Overhauser spectroscopy; CT, charge transfer; dmso, dimethylsulfoxide; OSSO, dimethylbis(methylsulfinylmethyl)silane; LMCT, ligand-to-metal charge transfer; MLCT, metal-to-ligand charge transfer

REFERENCES

(1) Andreasson, J.; Pischel, U.; Straight, S. D.; Moore, T. A.; Moore, A. L.; Gust, D. *J. Am. Chem. Soc.* **2011**, *133*, 11641.
(2) Dieckmann, V.; Eicke, S.; Springfeld, K.; Imlau, M. *Materials* **2012**, *5*, 1155.
(3) Gust, D.; Andreasson, J.; Pischel, U.; Moore, T. A.; Moore, A. L. *Chem. Commun.* **2012**, *48*, 1947.
(4) Al-Atar, U.; Fernandes, R.; Johnsen, B.; Baillie, D.; Branda, N. R. *J. Am. Chem. Soc.* **2009**, *131*, 15966.
(5) Wilson, D.; Branda, N. R. *Angew. Chem., Int. Ed.* **2012**, *51*, 5431.
(6) Kosa, T.; Sukhomlinova, L.; Su, L. L.; Taheri, B.; White, T. J.; Bunning, T. J. *Nature* **2012**, *485*, 347.
(7) Zhu, L. Y.; Al-Kaysi, R. O.; Bardeen, C. J. *J. Am. Chem. Soc.* **2011**, *133*, 12569.
(8) Morimoto, M.; Irie, M. *J. Am. Chem. Soc.* **2010**, *132*, 14172.
(9) Priimagi, A.; Shimamura, A.; Kondo, M.; Hiraoka, T.; Kubo, S.; Mamiya, J.-I.; Kinoshita, M.; Ikeda, T.; Shishido, A. *ACS Macro Lett* **2012**, *1*, 96.
(10) Terao, F.; Morimoto, M.; Irie, M. *Angew. Chem., Int. Ed.* **2012**, *51*, 901.
(11) Jin, Y.; Paris, S. I. M.; Rack, J. J. *Adv. Mater.* **2011**, *23*, 4312.
(12) McClure, B. A.; Rack, J. J. *Eur. J. Inorg. Chem.* **2010**, 3895.
(13) Rack, J. J. *Z. Kristallogr.* **2008**, *223*, 356.
(14) Rack, J. J. *Coord. Chem. Rev.* **2009**, *253*, 78.
(15) Brayshaw, S. K.; Easun, T. L.; George, M. W.; Griffin, A. M. E.; Johnson, A. L.; Raithby, P. R.; Savarese, T. L.; Schiffers, S.; Warren, J. E.; Warren, M. R.; Teat, S. J. *Dalton Trans.* **2012**, *41*, 90.
(16) Coppens, P.; Novozhilova, I.; Kovalevsky, A. *Chem. Rev.* **2002**, *102*, 861.
(17) Cormary, B.; Ladeira, S.; Jacob, K.; Lacroix, P. G.; Woike, T.; Schaniel, D.; Malfant, I. *Inorg. Chem.* **2012**, *51*, 7492.
(18) Hatcher, L. E.; Warren, M. R.; Allan, D. R.; Brayshaw, S. K.; Johnson, A. L.; Fuertes, S.; Schiffers, S.; Stevensen, A. J.; Teat, S. J.; Woodall, C. H.; Raithby, P. R. *Angew. Chem., Int. Ed.* **2011**, *50*, 8371.
(19) Heilwel, E. J.; Johnson, J. O.; Mosley, K. L.; Lubet, P. P.; Webster, C. E.; Burkey, T. J. *Organometallics* **2011**, *30*, 5611.
(20) Phillips, A. E.; Cole, J. M.; d'Almeida, T.; Low, K. S. *Inorg. Chem.* **2012**, *51*, 1204.
(21) Sheu, C.-F.; Shih, C.-H.; Sugimoto, K.; Cheng, B.-M.; Takata, M.; Wang, Y. *Chem. Commun.* **2012**, *48*, 5715.
(22) Sylvester, S. O.; Cole, J. M.; Waddell, P. G. *J. Am. Chem. Soc.* **2012**, *134*, 11860.
(23) Tahri, Z.; Lepski, R.; Hsieh, K. Y.; Bendeif, E. E.; Pillet, S.; Durand, P.; Woike, T.; Schaniel, D. *Phys. Chem. Chem. Phys.* **2012**, *14*, 3775.
(24) McClure, B. A.; Abrams, E. R.; Rack, J. J. *J. Am. Chem. Soc.* **2010**, *132*, 5428.
(25) Ciofini, I.; Daul, C. A.; Adamo, C. *J. Phys. Chem. A* **2003**, *107*, 11182.
(26) Gottle, A. J.; Dixon, I. M.; Alary, F.; Heully, J. L.; Boggio-Pasqua, M. *J. Am. Chem. Soc.* **2011**, *133*, 9172.
(27) Lutterman, D. A.; Rachford, A. A.; Rack, J. J.; Turro, C. *J. Phys. Chem. A* **2009**, *113*, 11002.
(28) Alessio, E.; Serli, B.; Zangrando, E.; Calligaris, M.; Panina, N. S. *Eur. J. Inorg. Chem.* **2003**, 3160.
(29) Calligaris, M. *Coord. Chem. Rev.* **2004**, *248*, 351.
(30) Kato, M.; Takayanagi, T.; Fujihara, T.; Nagasawa, A. *Inorg. Chim. Acta* **2009**, *362*, 1199.
(31) Mockus, N. V.; Rabinovich, D.; Petersen, J. L.; Rack, J. J. *Angew. Chem., Int. Ed.* **2008**, *47*, 1458.
(32) Smith, M. K.; Gibson, J. A.; Young, C. G.; Broomhead, J. A.; Junk, P. C.; Keene, F. R. *Eur. J. Inorg. Chem.* **2000**, 1365.
(33) Sullivan, B. P.; Salman, D. J.; Meyer, T. J. *Inorg. Chem.* **1978**, *17*, 3334.
(34) Garner, R. N.; Joyce, L. E.; Turro, C. *Inorg. Chem.* **2011**, *50*, 4384.

(35) McClure, B. A.; Rack, J. J. *Inorg. Chem.* **2011**, *50*, 7586.
(36) Biner, M.; Burgi, H.-B.; Ludi, A.; Rohr, C. *J. Am. Chem. Soc.* **1992**, *114*, 5197.
(37) Rilemma, D. P.; Jones, D. S.; Levy, H. A. *Chem. Commun.* **1979**, 849.
(38) Collin, J.-P.; Jouvenot, D.; Koizumi, M.; Sauvage, J.-P. *Inorg. Chim. Acta* **2007**, *360*, 923.
(39) Janiak, C. *Dalton Trans.* **2000**, 3885.
(40) Mockus, N. V.; Petersen, J. L.; Rack, J. J. *Inorg. Chem.* **2006**, *45*, 8.
(41) Rack, J. J.; Mockus, N. V. *Inorg. Chem.* **2003**, *42*, 5792.
(42) Buback, J.; Kullmann, M.; Langhojer, F.; Nuemberger, P.; Schmidt, R.; Wurthner, F.; Brixner, T. *J. Am. Chem. Soc.* **2010**, *132*, 16510.
(43) Wallin, S.; Davidsson, J.; Modin, J.; Hammarstrom, L. *J. Phys. Chem. A* **2005**, *109*, 4697.
(44) Tamai, N.; Miyasaka, H. *Chem. Rev.* **2000**, *100*, 1875.
(45) Ward, C. L.; Elles, C. G. *J. Phys. Chem. Lett.* **2012**, *3*, 2995.
(46) Alessio, E. *Chem. Rev.* **2004**, *104*, 4203.
(47) Tomita, A.; Sano, M. *Inorg. Chem.* **1994**, *33*, 5825.
(48) Rachford, A. A.; Petersen, J. L.; Rack, J. J. *Inorg. Chem.* **2005**, *44*, 8065.
(49) Lutterman, D. A.; Rachford, A. A.; Rack, J. J.; Turro, C. *J. Phys. Chem. Lett.* **2010**, *1*, 3371.
(50) McClure, B. A.; Mockus, N. V.; Butcher, D. P.; Lutterman, D. A.; Turro, C.; Petersen, J. L.; Rack, J. J. *Inorg. Chem.* **2009**, *48*, 8084.
(51) Logunov, S. L.; Volkov, V. V.; Braun, M.; El-Sayed, M. A. *Proc. Natl. Acad. Sci.* **2001**, *98*, 8475.
(52) Zamyatin, A. V.; Gusev, A. V.; Rodgers, M. A. *J. Am. Chem. Soc.* **2004**, *126*, 15934.